EDGEWOOD

CHEMICAL BIOLOGICAL CENTER

U.S. ARMY RESEARCH, DEVELOPMENT AND ENGINEERING COMMAND

ECBC-TR-652

LASER INDUCED MILLIMETER WAVE FLUORESCENCE FROM BIO-MATERIALS

Raphael P. Moon

RESEARCH AND TECHNOLOGY DIRECTORATE

Boris Gelmont

UNIVERSITY OF VIRGINIA
Charlottesville, VA 22908

Ashish Tripathi

SAIC

SCIENCE APPLICATIONS
INTERNATIONAL CORPORATION
Abingdon, MD 21009

October 2008

ABERDEEN PROVING GROUND, MD 21010-5424

Disclaimer

The findings in this report are not to be construed as an official Department of the Army position unless so designated by other authorizing documents.

REPORT DOCUMENTATION PAGE

Form Approved
OMB No. 0704-0188

1. REPORT DATE *(DD-MM-YYYY)*	2. REPORT TYPE	3. DATES COVERED *(From - To)*
XX-10-2008	Final	Oct 2005 - Sep 2007

4. TITLE AND SUBTITLE
Laser Induced Millimeter Wave Fluorescence from Bio-Materials

5a. CONTRACT NUMBER

5b. GRANT NUMBER

5c. PROGRAM ELEMENT NUMBER

6. AUTHOR(S)
Moon, Raphael P. (ECBC); Gelmont, Boris (UVA); and Tripathi, Ashish (SAIC)

5d. PROJECT NUMBER
BA06DET084

5e. TASK NUMBER

5f. WORK UNIT NUMBER

7. PERFORMING ORGANIZATION NAME(S) AND ADDRESS(ES)
DIR, ECBC, ATTN: AMSRD-ECB-RT-DL, APG, MD 21010-5424
University of Virginia, ECE Department, Charlottesville, VA 22908
SAIC, 3465A Box Hill Corporate Drive, Abingdon, MD 21009

8. PERFORMING ORGANIZATION PORT NUMBER
ECBC-TR-652

9. SPONSORING / MONITORING AGENCY NAME(S) AND ADDRESS(ES)

10. SPONSOR/MONITOR'S ACRONYM(S)

11. SPONSOR/MONITOR'S REPORT NUMBER(S)

12. DISTRIBUTION / AVAILABILITY STATEMENT
Approved for public release; distribution is unlimited.

13. SUPPLEMENTARY NOTES

14. ABSTRACT
In this report, we conduct the initial theoretical investigation of emission of radiation by DNA components upon the absorption of infrared (IR) radiation. Excitation wavelengths in 9 and 11 μm region are of interest. These transitions are related to the bond vibrations including only small groups of atoms. Hence, it is possible to analyze different fragments of DNA for identification of proper transitions. The carbon dioxide (CO_2) laser was chosen as the IR radiation source. We calculated the vibrational spectra of various DNA bases: cytosine; thymine; adenine; and guanine along with 2' deoxyadenosine 5'-monophosphate (dAMP); 2' deoxyguanosine 5'-monophosphate (dGMP); 2' deoxycytidine 5'-monophosphate (dCMP); 2' deoxythymidine 5'-monophosphate (dTMP) with HF/6-31G (d); and B3LYP approximation. The theoretical model considers the molecule as a system of coupled oscillators. The anharmonicity couples the oscillators and drives the energy transfer. Anharmonicity triggered transitions are analyzed. The Fermi resonances provide the most effective channels of the energy transfer. The probabilities of Fermi resonance induced transitions are calculated for the absorption bands evaluated with the HF model. We also acquired absorption spectra of DNA components from a herring sperm DNA sample. The tunable CO_2 laser induced emission spectra of these bio-chemicals was also acquired.

15. SUBJECT TERMS
Millimeter wave, Laser, DNA, Fermi, Resonances, Fluorescence, Absorption, Transmission, Oscillators

16. SECURITY CLASSIFICATION OF:			17. LIMITATION OF ABSTRACT	18. NUMBER OF PAGES	19a. NAME OF RESPONSIBLE PERSON
a. REPORT	b. ABSTRACT	c. THIS PAGE			Sandra J. Johnson
U	U	U	UL	30	19b. TELEPHONE NUMBER *(include area code)* (410) 436-2914

Blank

PREFACE

The work described in this report was authorized under Project No. BA06DET084. The work was started in October 2005 and completed in September 2007.

The use of either trade or manufacturers' names in this report does not constitute an official endorsement of any commercial products. This report may not be cited for purposes of advertisement.

This report has been approved for public release. Registered users should request additional copies from the Defense Technical Information Center; unregistered users should direct such requests to the National Technical Information Service.

Acknowledgment

The authors acknowledge Dr. Dwight Woolard (U.S. Army Research Office, Research Triangle Park, NC) for his technical support and guidance in this research work.

Blank

CONTENTS

FIGURES

TABLES

Blank

LASER INDUCED MILLIMETER WAVE FLUORESCENCE FROM BIO-MATERIALS

1. BACKGROUND

In recent years, the field of Terahertz (THz) science and technology has entered a phase of unprecedented expansion [1]. One of the major motivations for this renewed interest is the possibility of using THz spectral information for defense and security applications. Indeed, the demonstration of the THz vibrational spectra associated with biological molecules by prior U.S. Army and Defense Threat Reduction Agency (DTRA) supported research projects has been important for a number of reasons. For example, the very far-infrared (FIR) region of the DNA absorption spectra, 3-100 cm^{-1} (or 0.1-3 THz), has been shown to reflect the low frequency molecular internal motions. In this range, the spectral features from bio-polymer molecules arise out of poorly localized low-frequency molecular internal vibrations such as twisting, bending and stretching of the double helix, sugar pseudo-rotational vibrations and fluctuations of weakest bonds or non-bonded interactions (van der Waals forces, dispersion forces, and hydrogen bonding). The internal motions, dependent on the weak hydrogen bonds of the double-helix base-pairs, are extremely sensitive to DNA composition and topology and have an impact on the main processes related to the transfer of genetic information, such as replication, transcription and viral infection. Hence, phonon modes that arise in this range can reflect features specific to the DNA code. In addition, theoretical studies have predicted the occurrence of DNA phonon frequencies throughout this region and many have been linked directly to experimental data. Therefore, the continued investigation of the FIR region of the DNA absorption spectra for identifying DNA low-frequency internal motions are direct ways to obtain information about the peculiarities of DNA topology and internal motion. Furthermore, THz spectroscopy, coupled with theoretical prediction, can become a powerful tool for the investigation of the DNA structure and possible biological function.

During the last decade, the U.S. Army and DTRA have made a significant investment [2,3] in research aimed at investigating the potential use of THz frequency spectroscopy as a technique for the detection, identification, and characterization of biological agents. As is often typical, this research program was actually initiated by a very small exploratory investigation [3] into the THz-frequency absorption characteristics of fundamental bioagents (e.g., DNA). Over time, this research program has broadened into a wide-ranging multidisciplinary effort to address numerous challenges in the THz sensing-science and electronic-technology arenas [4, 5]. The overwhelming motivation for these THz activities clearly arose out of the anticipated impact they might have on identifying and developing effective sensor countermeasures against bio-warfare agent threats – in particular an effective bio-threat early-warning (e.g., standoff) capability, which historically has been one of the highest-priority goals of the relevant leadership in the Department of Defense (DoD) [6, 7]. The U.S. Army and other DoD agencies have been particularly active in the support of scientific research into THz bio-signature phenomenology using Fourier Transform Infrared (FTIR) [8] and photo mixer [9] based technology, both of which possess the high sensitivity to measure the weak absorption features associated with biomaterials. In fact, a continuous and focused effort on THz sensing phenomenology in DNA and related biological materials [8, 10] was used to produce credible experimental evidence for the existence of species-specific resonance features that arise from phonon mode activity at the molecular level. These demonstrations are important

because they validate earlier theoretical predictions of a link between THz resonances and internal structure (e.g., dependent on hydrogen bonds of the double-helix base-pairs), and therefore defined a spectroscopic approach for interrogating microscopic information (e.g., genetic information encoded in the variety and arrangement of DNA nucleotides) that could be useful for bio-agent detection and analysis. Fourier transform (FT) transmission (absorption) spectroscopy has provided to this point the most detailed information on THz vibrational spectral signatures of biological molecules. The measurement of these THz spectral signatures is very difficult due to their relatively weak strength. Yet there has been independent confirmation under varying laboratory conditions [9], along with system-level studies [7,11,12], and theoretical predictions that these same THz-signatures are viable for use in medium-range remote-detection of bio-particles. Hence, this research clearly suggests potential payoffs for THz sensing and imaging in the biological and medical sciences and in other closely related military applications [1]. Numerous difficulties make the direct identification of THz phonon modes in biological materials very challenging. The THz vibrational spectroscopy has demonstrated [8] that such measurements can be effective and fruitful. Spectra of different DNA samples reveal a large number of modes and a modest level of sequence-specific uniqueness. These internal motions are sensitive to DNA composition and topology. They have an impact on the main processes related to the transfer of genetic information and eventually can give information regarding the three dimensional structure and flexibility of the DNA double helix. Hence, these prior successes motivate the investigations of new methodologies for the more efficient collection of long wavelength spectral information from biological materials and agents. As part of a joint project between the U.S. Army Edgewood Chemical Biological Center (ECBC) and the University of Virginia, a new approach to detecting and identifying DNA is being investigated that is based upon the premise that the DNA will radiate millimeter wave (MMW) and/or sub-millimeter wave (sub-MMW) energy upon the absorption of infrared (IR) radiation. The proposed hypothesis assumes that the excitation of molecular vibrations in the DNA by the application of laser energy, at known IR absorption peaks, can lead to the production of low frequency (MMW and/or THz) radiation from the DNA through nonlinear phonon-decay processes. If this hypothesis is valid, and there is certainly evidence to suggest that this could be possible as elemental units of DNA are known to exhibit strong absorption in the IR. The resulting long wavelength fluorescence should provide a much more effective methodology for probing the allowed vibrational modes associated with biological agents of interest.

2. OVERVIEW

This approach can be visualized as a FIR fluorescence of biological molecules. The IR radiation can excite the vibrational bonds. It is possible that vibrational relaxations may result in energy emission into lower (sub-millimeter and millimeter) spectral regions. This long wavelength fluorescence might be an alternative approach to bio-detection. The millimeter/sub-millimeter-wave frequency regime is expected to have multiple spectral features that are dependent on DNA internal vibrations. The vibrations are spread over large portions of the complex molecule. Thus, spectral emission dependent on the primary sequence of the molecule may be expected [10]. The acquisition of millimeter/sub-millimeter-wave spectroscopy is limited due to low absorption of THz radiation by the DNA molecule. Therefore, it is desirable to investigate non-THz region radiation absorption pathways that may result in THz region emission spectra. In other words, our plan is to look for "other than THz excitation source" to obtain emission spectra in THz region. In this work, we conducted the initial theoretical

investigation of emission of radiation by DNA upon the absorption of powerful IR radiation. We studied the anharmonicity of different transitions that are responsible for the vibrational energy transfer from IR region to lower frequencies. Fermi resonance is such an energy transition pathway. We performed the vibrational analyses of four different monophosphates including deoxycytidine 5'-monophosphate (dCMP); deoxythymidine 5'-monophosphate (dTMP); deoxyadenosine 5'-monophosphate (dAMP); and deoxyguanosine 5'-monophosphate (dGMP). These vibrational analyses were within the Hartree-Fock approximation and the density functional theory (DFT) in G03W packages. Initially the IR absorption bands must be evaluated. For each of the IR absorption band in 900 to 1100 cm^{-1} wavenumber region, the probability of Fermi resonance must then be estimated. If an IR absorption band indicates higher probability of energy transition via Fermi resonance, it indicates the possible occurrence of emission bands in the MMW region. An observable indicator of this transition is the occurrence of emission band at twice the wavelength of excitation radiation. An IR spectroscope can be used to confirm the presence of the emission band. If the emission band is observed, THz emission spectra may be observed at MMW region. Figure 1 shows a flow chart that describes our approach.

3. THEORETICAL VIBRATIONAL ANALYSES

Long-wavelength vibrational absorption (transmission) spectra may be used for detection of DNA molecule. The theoretical investigation of emission of millimeter/ sub-MMW radiation by DNA upon the absorption of IR radiation is the objective of this study. The carbon dioxide (CO_2) laser will be the candidate for the source of IR radiation; thus, the wavelengths in the region between 9 μm (~1100 cm^{-1}) and 11 μm (~900 cm^{-1}) are of interest. The output of a CO_2 laser is medium-IR radiation around a range near 10.6 μm wavelength. Therefore, possible light induced transitions have to be found at this wavelength. These transitions are related to the bond vibrations including only small group of atoms. Hence, it is possible to analyze different fragments of DNA for identification of possible transitions to MMW region upon the absorption of IR radiation. Therefore, the newly proposed approach requires a comprehensive theoretical analysis of the vibrational modes and interactions within the DNA molecular structure, as applied to millimeter wave emission. Such an analysis starts from development a theoretical model. We have begun with analyses of IR absorption by nitrogenous bases and then we studied absorption of monophosphates as it is known the single stranded DNA consists of nucleotides connected with each other via phosphates groups. We performed the vibrational analyses of four different monophosphates including deoxycytidine 5'-monophosphate (dCMP), deoxythymidine 5'-monophosphate (dTMP), deoxyadenosine 5'-monophosphate (dAMP), and deoxyguanosine 5'-monophosphate (dGMP). The vibrational analyses were within Hartree-Fock approximation and the density functional theory (DFT) in G03W [13] packages to estimate the absorption bands in the IR spectral region. The transfer absorbed IR energy is the key process for emission in MMW region. The proposed theoretical model considers the molecule of interest as a system of coupled oscillators. The emission is expected due to the energy transfer from one excited oscillator to another with lower frequency. Strong coupling is required for this process. Therefore, we study the anharmonicity of different transitions that are responsible for the vibrational energy transfer from IR region to lower frequencies.

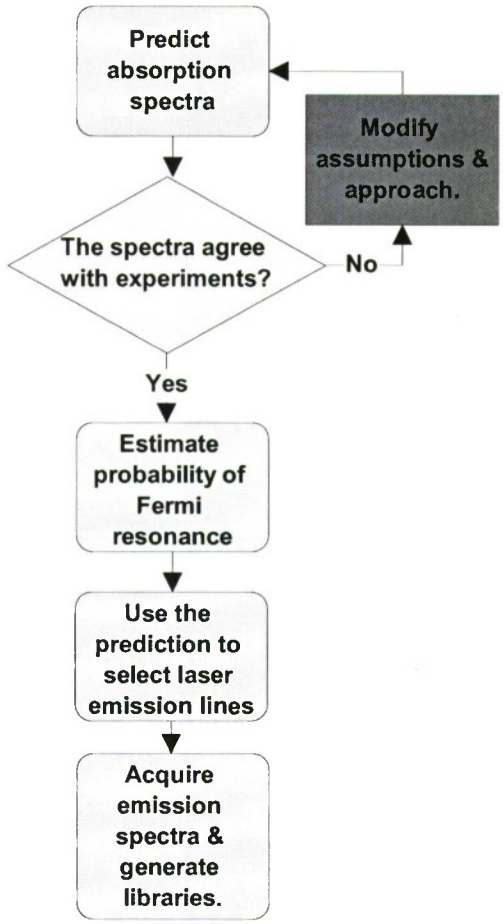

Figure 1. Outline of Our Approach to Obtaining THz Region Emission Spectra from an IR Excitation Source.

Fermi Resonance. The difficult part of the theoretical study is the analysis of the possible channels for transferring the energy associated with the IR excitation to the lower-energy (i.e., longer wavelength) vibrations. Anharmonicity is the cause of coupling of two nearly identical frequency (one of which is the excitation radiation) oscillators in complex molecules. The result of such coupling is the Fermi resonance, which may result in transfer of absorbed energy via multiples of absorbed excitation radiation wavelength. If the vibrational frequency coincides with the frequency of the laser radiation, transition from the ground state to the first excited level of the oscillator occurs under influence of the laser radiation. Such a picture is valid for harmonic oscillators when only the parabolic potential is taken into account. A brief discussion on parabolic potential is presented in the Appendix. Normal mode analysis of standard algorithms gives us possibility to find all available oscillator frequencies and to calculate probabilities of any transition. The selection rule for a harmonic oscillator states that transitions are allowable only between adjacent levels of the same oscillator. All transitions between different oscillators are forbidden. However, the vibrations of real molecules are not strictly harmonic, and the oscillators are coupled because of the anharmonicity. The potential is parabolic only in the lowest order of expansion into displacements of atoms. The anharmonicity is responsible for coupling of the oscillators and the energy transfer. We study a rather complex

molecule with many atoms. The potential is a function of 3N-6 variables where N is the number of atoms. To estimate the possible effect of nonparabolicity on oscillator coupling, some relatively simple approach has to be developed. In the lowest order of the expansion in the atomic displacements, δr, the nonparabolic part of the potential of the interaction between two atoms, v_{np}, is proportional to the third power of the displacements.

$$v_{np}(1,2) = (\frac{\partial^3 V}{\partial r^3})_0 \frac{((\delta\vec{r}(1) - \delta\vec{r}(2))(\vec{r}_0(1) - \vec{r}_0(2)))^3}{6 \mid \vec{r}_0(1) - \vec{r}_0(2) \mid^3} \tag{1}$$

We have taken into account only stretching of the bond. Hence only relative displacement of atoms is important. According to our approximation the total nonparabolic potential includes only interaction between nearest neighbors

$$V_{np} = \frac{1}{2}\sum_{k,l} v(k,l) \tag{2}$$

Such terms can be responsible for the coupling between the first excited state of one oscillator, which is populated as a result of the laser radiation, and the second excited states of the other oscillator. If the energy of these two states is close enough, the Fermi resonance occurs. The displacement of atomic coordinates is connected with eigenvectors of oscillators in the following way [14]:

$$\delta\vec{r}(k)\sqrt{M_k} = \sum_j \vec{s}(k \mid j) q_j \tag{3}$$

where $\vec{s}$ is Eigen vectors of oscillator j, qs are normal coordinates ,M_k is the atomic mass. The matrix element of the nonparabolic potential between two states of two oscillators, j and n, can be written as follows:

$$< j1; n0 \mid V_{np} \mid j0; n2 >= \frac{1}{4\omega_n \omega_j^{1/2} \mid \vec{r}_0(1) - \vec{r}_0(2) \mid^3} (\frac{\partial^3 V}{\partial r^3})_0$$

$$((\frac{\vec{s}(1 \mid j)}{M_1^{1/2}} - \frac{\vec{s}(2 \mid j)}{M_2^{1/2}})(\vec{r}_0(1) - \vec{r}_0(2)))((\frac{\vec{s}(1 \mid n)}{M_1^{1/2}} - \frac{\vec{s}(2 \mid n)}{M_2^{1/2}})(\vec{r}_0(1) - \vec{r}_0(2)))^2 \tag{4}$$

At first, we estimated the coupling of the oscillators using the first order of the perturbation theory. However, it proved that some oscillators are strongly coupled. In this case, we have taken into account an interaction only between these two oscillators. The energies of two coupled are renormalized

$$E_1 = [E(j1; n0) + E(j0; n2)]/2 + \Delta/2 \tag{5a}$$
$$E_2 = [E(j1; n0) + E(j0; n2)]/2 - \Delta/2 \tag{5b}$$

Energy level splitting of two renormalized levels Δ is as follows

$$\Delta = \{\delta^2 + 4 |< j1;n0 | V_{np} | j0;n >|^2\}^{1/2} \quad (6)$$

Splitting of unperturbed levels δ is determined by

$$\delta = | E(j1;n0) - E(j0;n2) | \quad (7)$$

The wave functions of two resulting states are

$$\psi_1 = a | j1;n0 > -b | j0;n2 > \quad (8a)$$

$$\psi_2 = b | j1;n0 > +a | j0;n2 > \quad (8b)$$

where

$$a = (\frac{\Delta + \delta}{2\Delta})^{1/2} \quad (9a)$$

$$b = (\frac{\Delta - \delta}{2\Delta})^{1/2} \quad (9b)$$

As a result, the transition occurs between the $| j1;n0 >$ state of the oscillator j and $| j0;n2 >$ state of the oscillator n. The probability is proportional to $|b|^2$. The spontaneous emission from $| j0;n2 >$ state of the oscillator n to the first excited state and then to the ground state becomes possible and such fluorescence can be detected. Figure 2 shows a graphical representation of Fermi resonance.

4. EXPERIMENTAL PROCEDURES

The laser excitation source along with power attenuating and continuous-to-pulsed mode conversion optics was set-up. A continuous tune-able CO_2 laser (MTB model GN-802-GES) serves as the excitation source. The laser is capable of emitting 80 emission lines in 9.6 and 11.4 μm wavelength range. The laser power is controlled by a combination of polarization based attenuators and a ZnSe optics based beam expander (II-VI corp, Model 1755). The laser operates in continuous (CW) mode. The emission wavelength is measured with a CO_2 laser spectrum analyzer (Macken Instruments, Model 16 A).Three CO_2 laser emission lines were used as the excitation source – at 970 cm^{-1} (10.31 μm wavelength), at 1080 cm^{-1} (9.26 μm wavelength) and at 949 cm^{-1} wave number (10.54 μm wavelength). Transmission Fourier Transformed Infrared (FTIR) spectra were obtained while exposing the sample to these laser lines with a FTIR spectrometer (Newport Instrument Model MIRAMAT 8025) coupled with a Deuterated tri-glycine sulfate (DTGS) pyroelectric detector (Newport Instrument model 80008). Figure 3 shows the experimental setup. Genetic components such as adenosine, guanosine, dAMP, dGMP, dCMP, and Herring sperm DNA were dissolved or suspended at 20 mg/mL concentration in de-ionized water. An aliquot (1 mL) of the prepared aqueous solution or

suspension was coated on a 1.5 in. diameter, 5 mm uncoated ZnSe window. Upon drying, a film residue of the dissolved or suspended chemical remained on the ZnSe window. FTIR spectra of the prepared chemicals samples were obtained with a SiC IR source (Newport Model 80007).

The sample on ZnSe window was exposed to the laser. The sample side of the ZnSe window faced the FTIR instrument. This is because ZnSe is transparent to IR radiation up to 20 μm only. The CW mode of operation may result in thermal energy build up in the sample. Laser power density was optimized with the polarizer attenuators and beam expander to maximize FTIR signal strength without causing any thermal induced damage to the sample (Herring Sperm DNA). The lack of damage was ascertained by examining the FTIR spectra of the sample before and after exposer to the laser. The FTIR spectra obtained before the exposer to CW laser matched with that obtained after the exposer to CW laser.

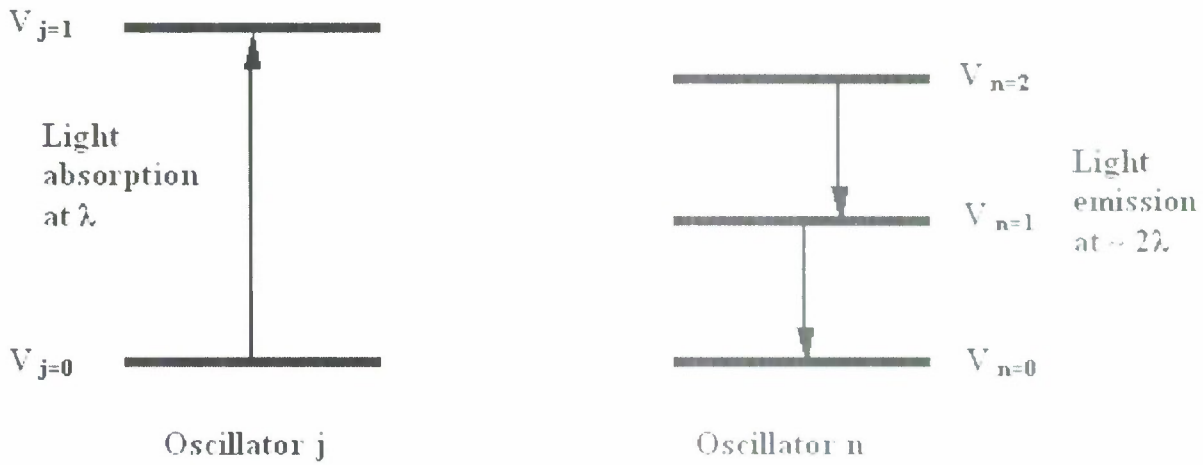

Figure 2. Fermi Resonance is a Splitting of Lines in an Infrared Spectrum. It occurs when two vibrational states of a molecule have different modes of movement but almost the same energy.

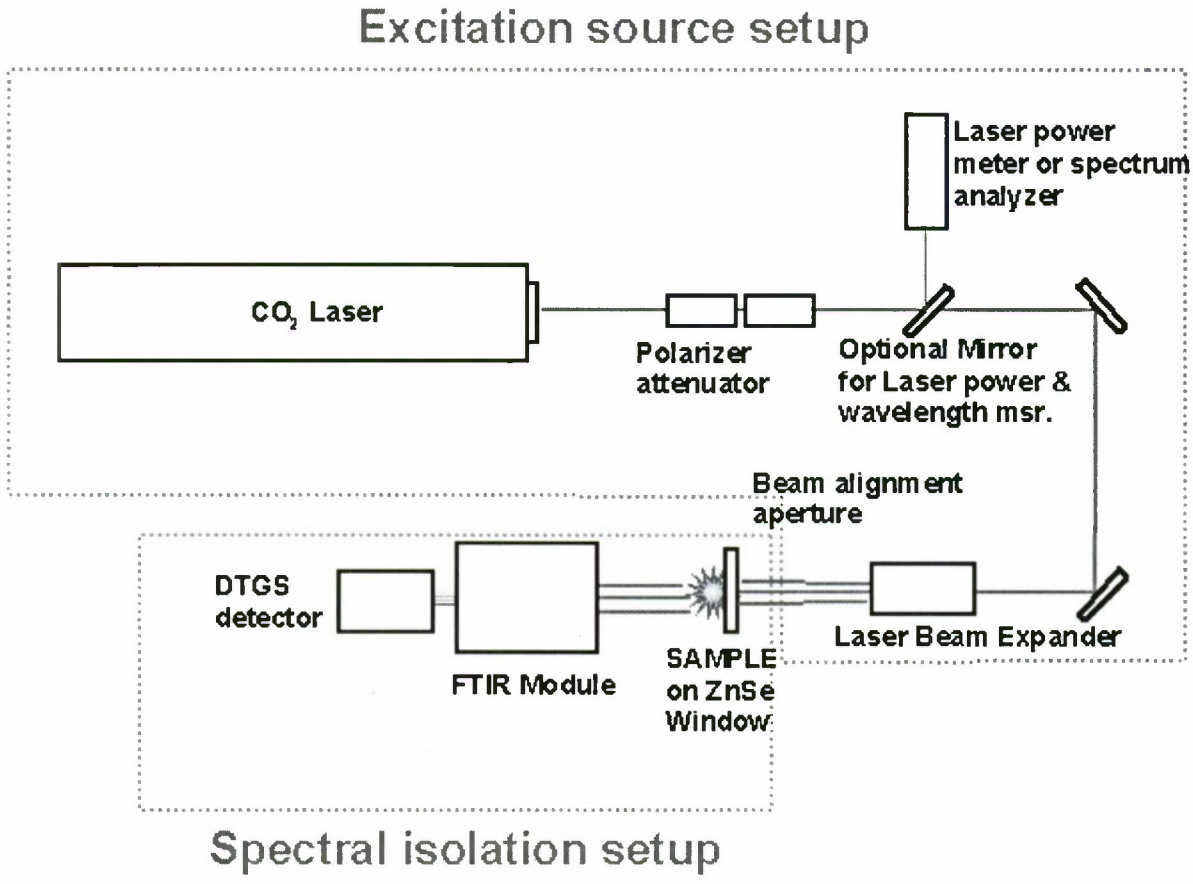

Figure 3. Experimental Setup for Spectral Acquisition

5. RESULTS AND DISCUSSIONS

For our simulations, we used a single molecule of dAMP sodium salt (Figure 4). The structure was optimized on DTF using wave functions B3LYP/6-31G(d) and HF/6-31G(d) level of theory. The optimized using B3LYP and HF structures look quite similar (Figure 4). We also calculated vibrational spectrum and IR absorption peak intensities for these two models. While the results are somewhat comparable, it is impossible to scale HF IR peaks on the frequency scale to match B3LYP IR peaks in a broad frequency range since HF frequency range is broader than B3LYP frequency range. To compare our simulations with measured transmission data on dAMP sodium salt, we plotted our theoretical peak positions versus $\log(I_w/I_{dAMP})$, where I_w is the transmitted intensity for ZnSe window, and I_{dAMP} is the transmitted intensity for ZnSe window with dAMP sodium salt on it. The most important range for comparison with the theory is 600-1200 cm^{-1} (Figure 5). Density Functional Theory (pink drop lines) provides more consistent agreement with experiment (Figure 2) than HF (cyan drop lines). Analogous simulations were made for a single molecule of dCMP sodium salt (Figure 6). The structure was optimized on DTF using wave functions B3LYP/6-31G(d) and HF/6-31G(d) level of theory. The optimized B3LYP and HF structures look quite similar (Figure 7). We also calculated vibrational spectrum and IR absorption peak intensities for these two models. Although the results are somewhat comparable, it is impossible to scale HF IR peaks on the frequency scale to match B3LYP IR peaks in a broad frequency range because HF frequency

range is broader than B3LYP frequency range. To compare our simulations with measured transmission data on dCMP sodium salt, we plotted our theoretical peak positions versus $\log(I_w/I_{dAMP})$, where I_{dAMP} is a transmitted intensity for ZnSe window with dCMP sodium salt on it. The sharpest resonant features are observed in 800-1800 cm^{-1}. Figure 2 shows comparison of modeling results with experimental data in 700-1800 cm^{-1} frequency range. Density Functional Theory (pink drop lines) provides more consistent agreement with the experiment than HF (cyan drop lines). However, in some instances scaled HF is closer to the experiment (for example, the absorption peak at 1045 cm^{-1}).

B3LYP/6-31G(d) HF/6-31G(d)

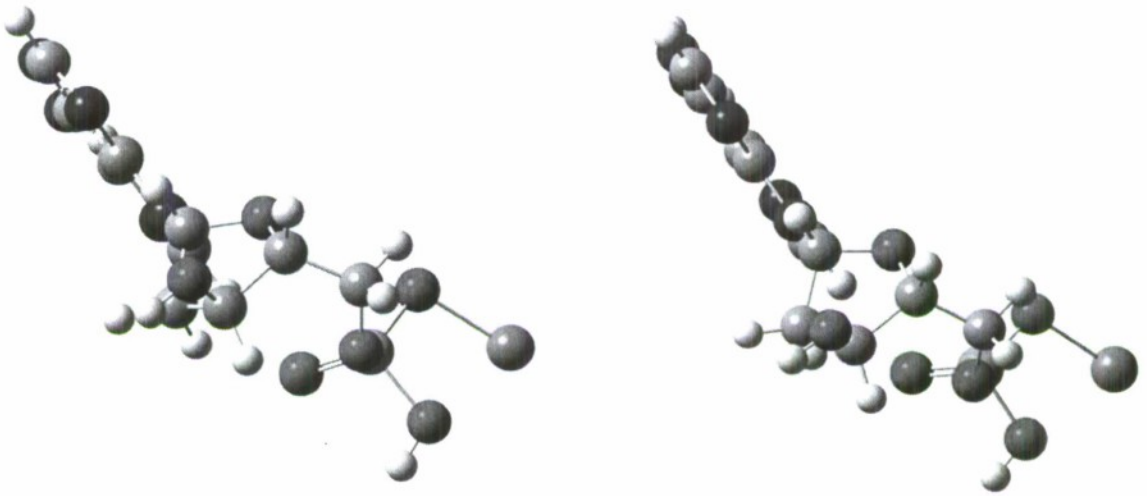

Figure 4. dAMP – Na Optimized Using B3LYP (left) and HF (right) Structures

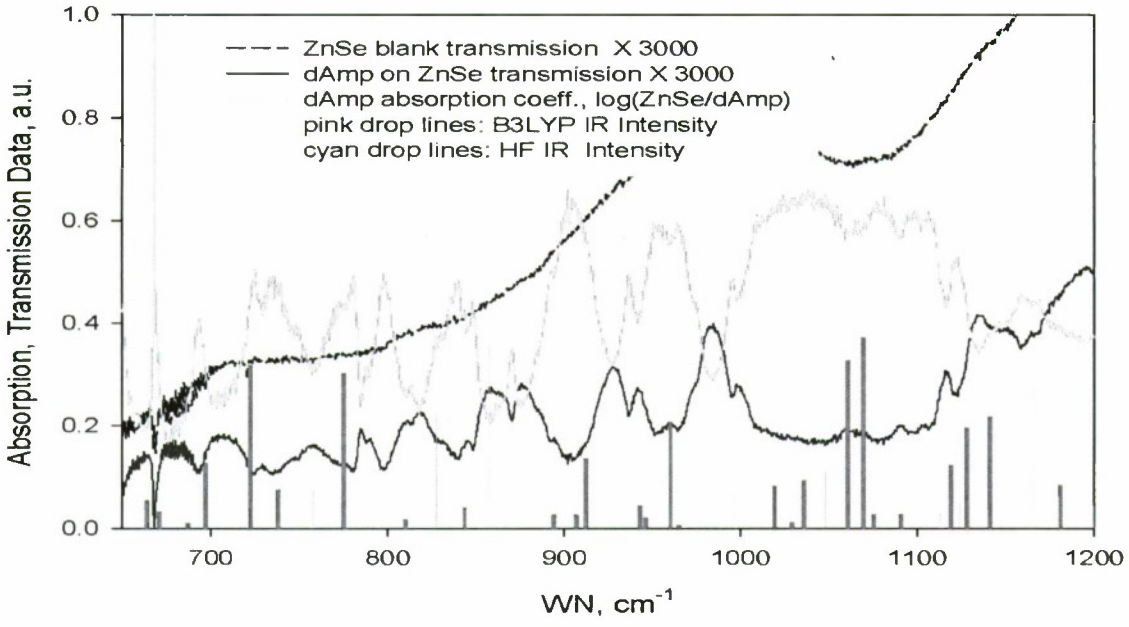

Figure 5. Experimental dAMP – Na transmission (blue dots), dAMP Absorption (green), ZnSe Transmission (grey). Theoretical IR Intensity HF (cyan drop lines), B3LYP (pink drop lines)

B3LYP/6-31G(d)
Dipole moment 8.85 Debye
Energy -1545.411 a.u.

HF/6-31G(d)
Dipole moment 9.91 Debye
Energy -1538.524 a.u.

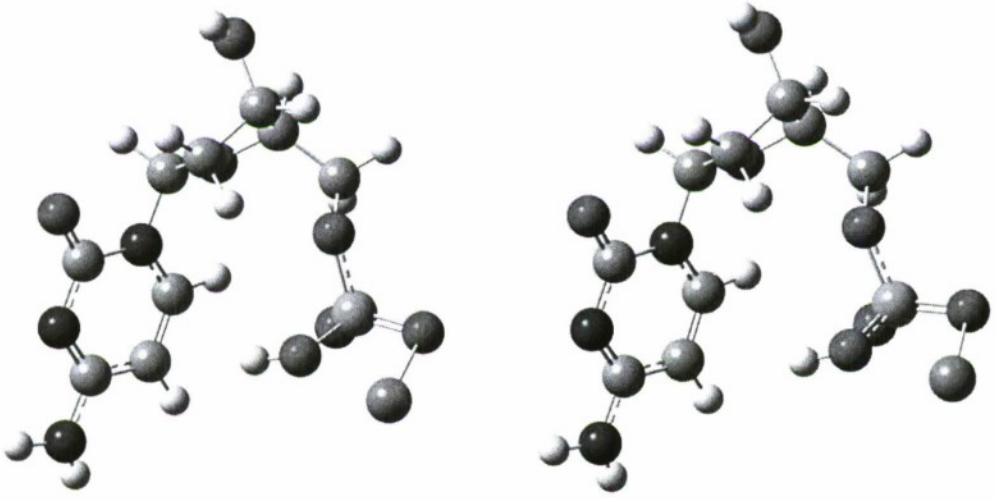

Figure 6. dCMP – Na Optimized Using B3LYP (left) and HF (right) Structures

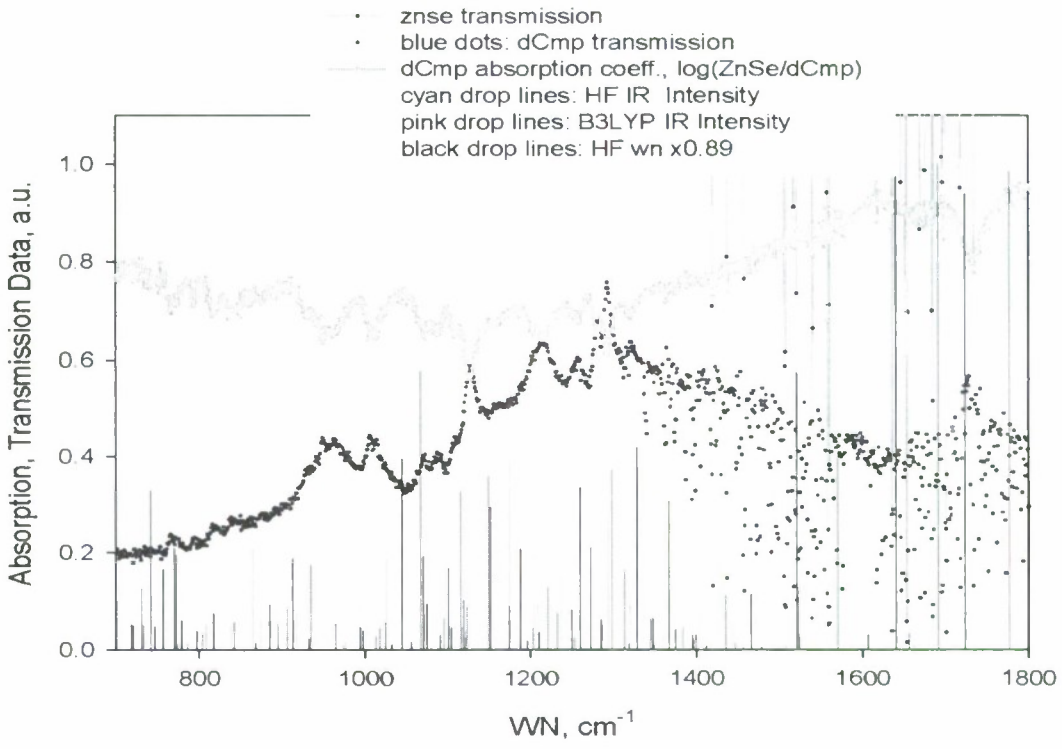

Figure 7. Experimental dCmp Transmission (blue dots), dCmp Absorption (green), ZnSe Transmission (grey). Theoretical IR intensity HF Unscaled (cyan drop lines), HF Scaled by 0.89 (black drop lines); B3LYP (pink drop lines).

Following the discussion on Fermi resonance, we have also calculated the probability of transitions from the first excited level of oscillator j with fundamental vibrational frequencies around 1000 cm^{-1} to the second excited level of oscillator j' with fundamental vibrational frequency half of oscillator j. Vibrational frequencies of normal modes of dAMP, dCMP, dGMP, and dTMP in the region between 900 cm^{-1} and 1100 cm^{-1} are listed in Table 1-4 with the infrared intensity and transition probability. The IR intensity and transition probability are two important parameters to determine the possible coupling. Those normal modes with strong IR intensity and large transition probability are mostly possible to be coupled. To compare the IR intensity and transition probability of different oscillators, we plot the transition probability and ratio by dividing the IR intensity by maximal IR intensity of all modes for one monophosphate. As shown in Figure 8 (a)-(d), 927.8 and 1091.0 cm^{-1} in dAMP, 928.2 cm^{-1} in dCMP, 1092 cm^{-1} in dGMP, and 928.5 and 1066.3 cm^{-1} in dTMP have relatively strong IR intensity and large transition probability, so the emission of oscillators with fundamental frequencies about half of these frequencies may possibly be detected (i.e., 447.0 and 545.6 cm^{-1} in dAMP, 454.4 cm^{-1} in dCMP, 1063.5 cm^{-1} in dGMP, and 480.5 and 534.4 cm^{-1} in dTMP).

Table 1. dAMP

Frequency of oscillator j (cm^{-1})	Frequency of oscillator n (cm^{-1})	IR Intensity of oscillator j (km/mole)	Transition Probability from j to n
893.3715	447.0434	10.5600	0.4987
905.5862	447.0434	84.8400	0.4923
927.8362	447.0434	450.2500	0.4889
937.4387	481.5760	82.3500	0.4187
943.5008	483.4127	15.5400	0.3569
990.3927	498.5691	24.4100	0.4946
1005.4606	498.5691	50.0200	0.4821
1006.0393	498.5691	38.9500	0.4760
1021.5098	483.4127	73.2300	0.4855
1036.2056	517.9103	67.7200	0.4993
1042.6996	517.9103	16.6200	0.4890
1043.6571	517.9103	70.8100	0.4853
1067.1305	545.5873	154.4400	0.4850
1090.9962	545.5873	319.5600	0.4992
1107.0922	558.4371	107.0000	0.4567

Table 2. dCMP

Frequency of oscillator j (cm^{-1})	Frequency of oscillator n (cm^{-1})	IR Intensity of oscillator j (km/mole)	Transition Probability from j to n
888.5167	436.3864	88.9	0.4371
905.0980	454.3608	171.6200	0.4856
928.2389	454.3608	401.5500	0.4737
951.3957	480.2194	40.0355	0.3821
955.8588	480.2194	74.0594	0.3688
1008.5128	485.9967	2.9045	0.2670
1019.3473	514.7401	93.6964	0.2932
1024.9673	454.3608	88.3827	0.3947
1037.5852	454.3608	17.4564	0.3436
1054.1155	546.0317	489.8660	0.2844
1059.3435	514.7401	164.7650	0.1253
1082.1600	546.0317	91.67	0.4527

Table 3. dGMP

Frequency of oscillator j (cm^{-1})	Frequency of oscillator n (cm^{-1})	IR Intensity of oscillator j (km/mole)	Transition Probability from j to n
884.4023	447.2353	111.72	0.4506
905.7341	447.2353	91.2600	0.4785
911.3060	481.4115	459.7730	0.0966
928.9287	484.6788	74.6400	0.4267
938.2027	473.8651	43.0000	0.4378
1001.5128	481.4115	74.3300	0.4310
1009.8731	484.6788	85.3200	0.4599
1018.7899	481.4115	99.6000	0.4783
1037.5867	481.4115	34.3305	0.4604
1041.9517	481.4115	95.6000	0.2948
1050.9014	543.3867	42.0100	0.4526
1063.4833	543.3867	341.75	0.4801
1080.8401	543.3867	109.055	0.4979

Table 4. dTMP

Frequeney of oscillator j (cm^{-1})	Frequeney of oseillator n (cm^{-1})	IR Intensity of oscillator j (km/mole)	Transition Probability from j to n
885.9752	450.7559	118.45	0.4430
908.0873	450.7559	113.3700	0.4903
928.5404	480.5016	416.0200	0.4180
952.4650	480.5016	40.3500	0.4755
966.2100	468.7759	13.2600	0.3918
1006.1159	480.5016	80.8700	0.4536
1012.4520	534.4268	8.0400	0.4115
1023.8976	480.5016	83.8700	0.4690
1041.0482	480.5016	82.7900	0.4739
1056.7411	534.4268	27.1000	0.4758
1063.4948	547.5815	54.4900	0.3558
1066.2629	534.4268	10.9400	0.4479
1082.8940	534.4268	376.8600	0.4895
1098.8153	547.5815	115.65	0.4957
1112.0538	547.5815	87.46	0.4083

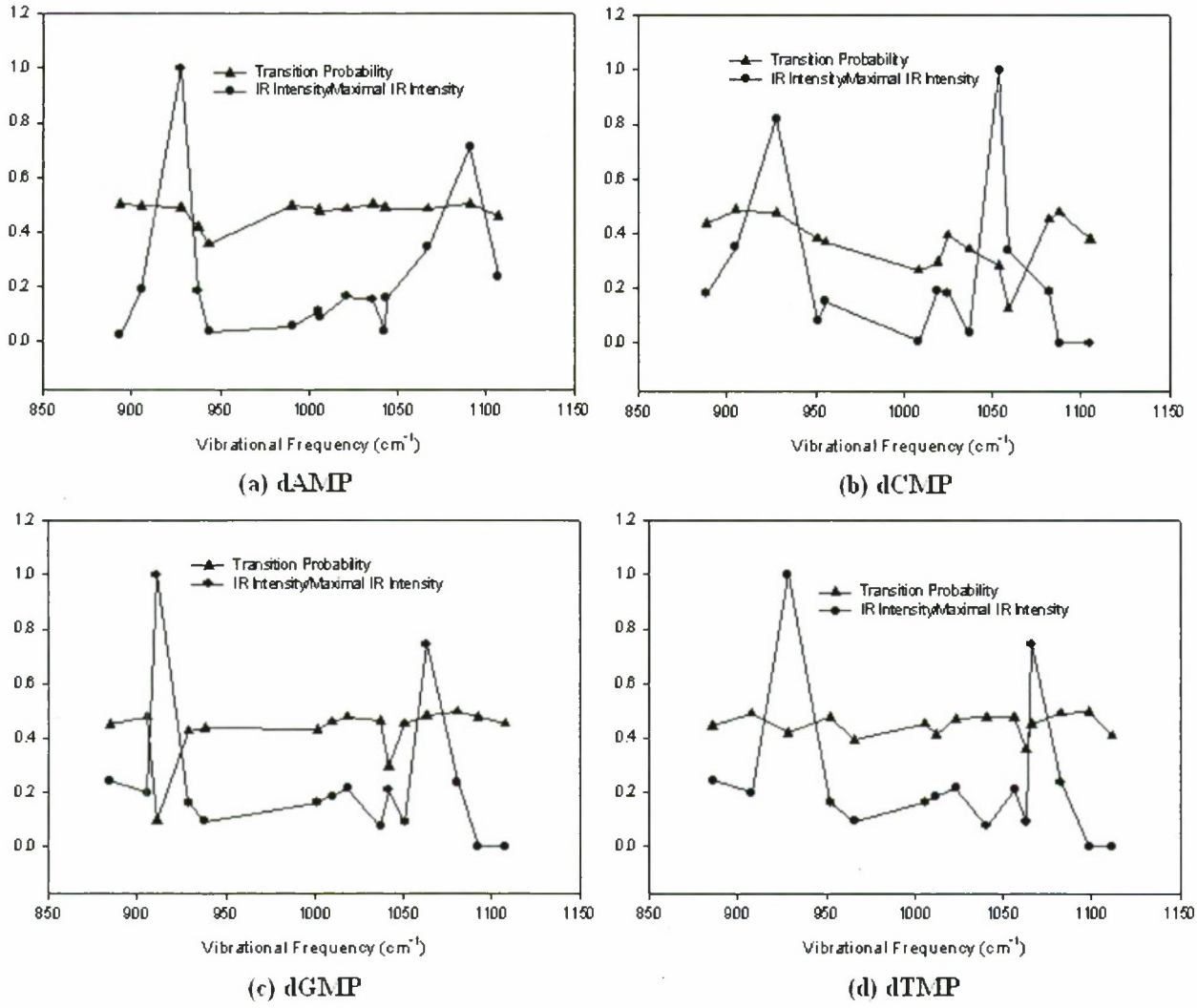

Figure 8. Plots of IR Intensity/Maximal IR Intensity of Different Vibrational Modes j and Transition Probability from Oscillator j to Oscillator n: (a) dAMP; (b) dCMP; (c) dGMP; and (d) dTMP.

Fermi resonance modeling strongly suggests that a possibility of energy transfer to lower energy states exists. Thus, we conducted limited laser-excitation experiments. The samples coated on ZnSe windows were exposed to three different laser lines at 1080 cm^{-1} (9.26 μm wavelength) and at 949 cm^{-1} wavenumber (10.54 μm wavelength). A single spectrum was the result of 100 consecutive spectral co-adds for improved signal-to-noise ratio. Boxcar apodization technique was used to obtain the FTIR spectra. Figure 9-11 show the spectral response to the three laser lines. The region shaded in grey is the twice the incident radiation wavelength region. A small emission line (no more than 2 % of the incident laser line intensity), at twice the wavelength, was observed for most of the DNA components. Figure 9 shows strong emission peak at twice the wavelength (540 cm^{-1} wavenumber) for polystyrene, guanosine, and adenosine when excited with 1080 cm^{-1} laser line. Whereas, Figure 10 shows strong emission peak at twice the wavelength (485 cm^{-1} wavenumber) for guanosine , adenosine, and dGMP when excited with 970 cm^{-1} laser line. Figure 11 shows emission peak at twice the wavelength

(474 cm^{-1} wavenumber) for DNA, adenosine, and dGMP. Also a very strong emission peak for guanosine is observed at 474 cm^{-1} wavenumber when excited with 970 cm^{-1} laser line. Figure 12 shows the cumulative emissive spectral response from exposer to the three laser lines. The grey region shows the twice the incident radiation wavelength region. Clearly response from each of the sample is visually different from each other. This finding may indicate occurrence of Fermi resonance, which needs to be confirmed with computational modeling.

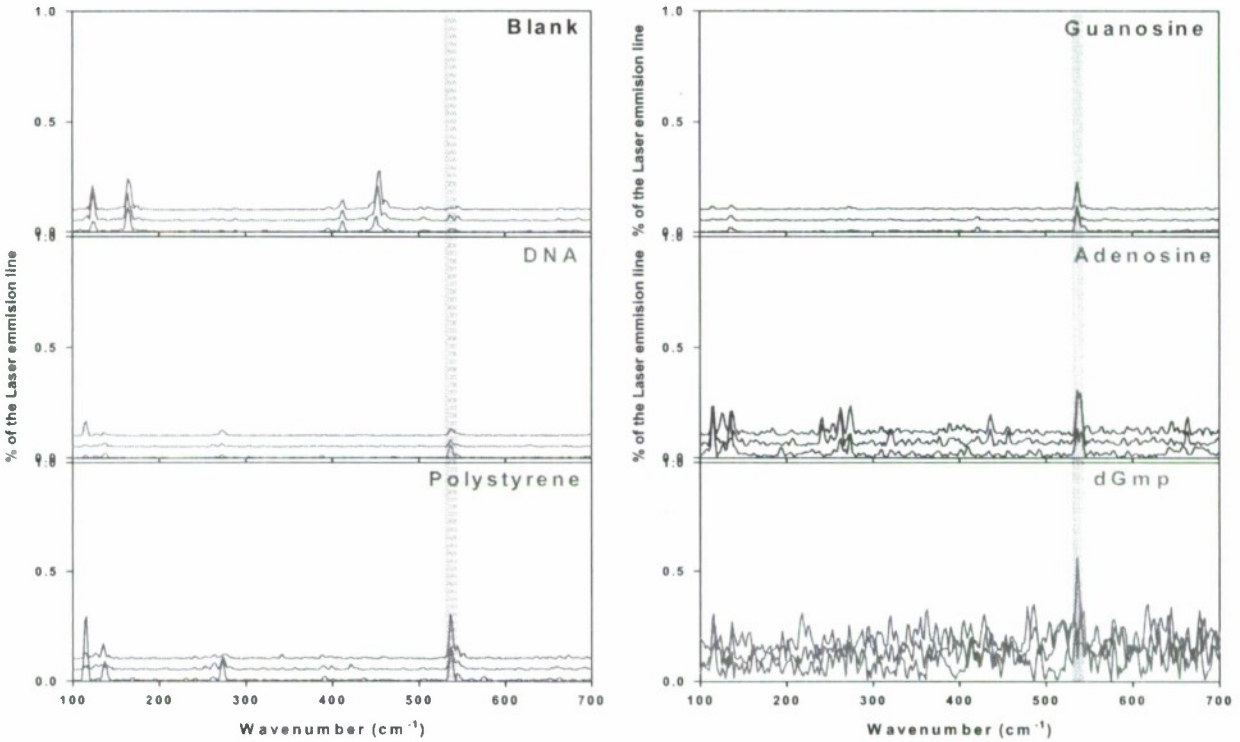

Figure 9. Emission/Transmission Spectra when Excited by 1080 cm^{-1} CO_2 Laser Line. Each spectrum is average of 100 spectra.

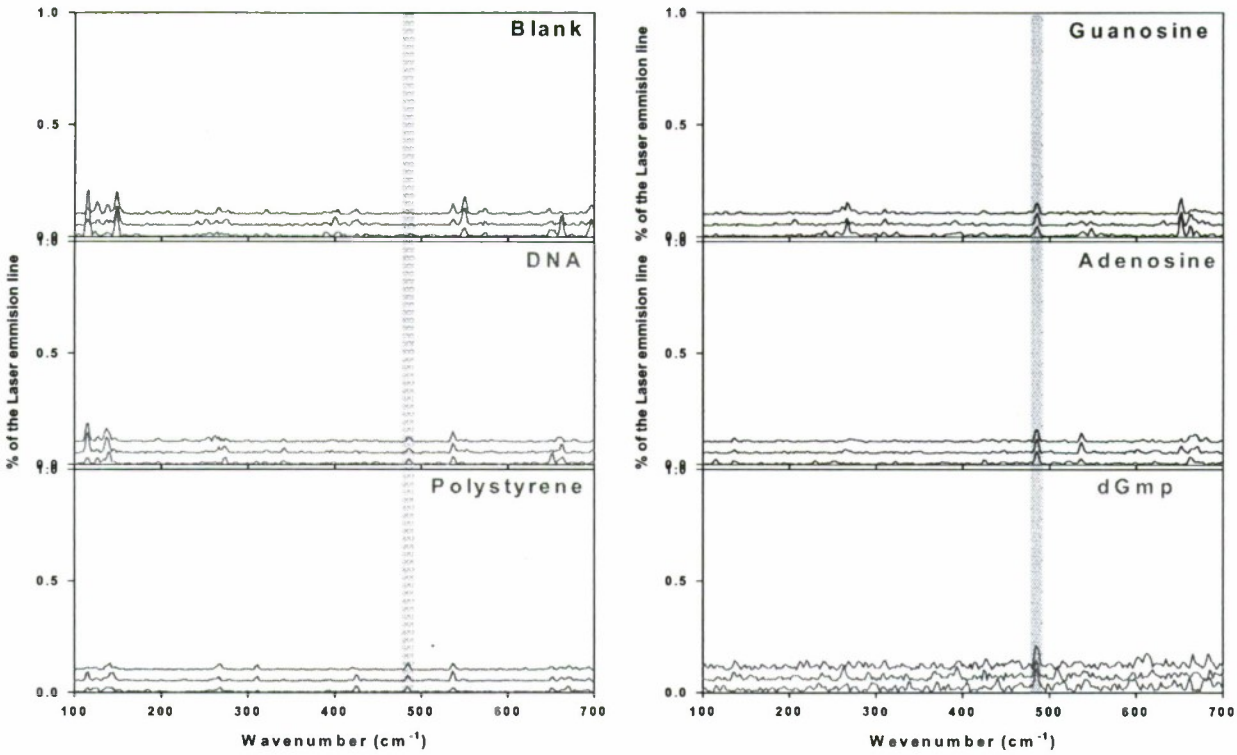

Figure 10. Emission/Transmission Spectra when Excited by 970 cm^{-1} CO_2 Laser Line. Each spectrum is average of 100 spectra.

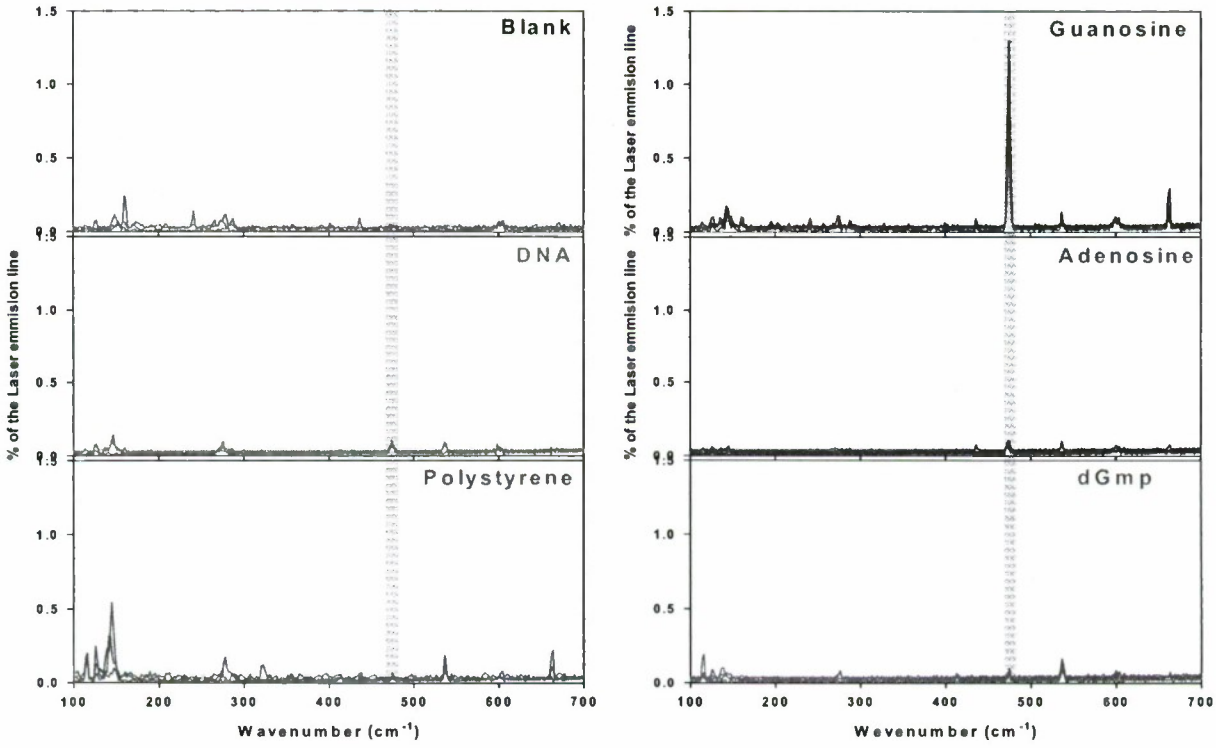

Figure 11. Emission/Transmission Spectra when Excited by 949 cm^{-1} CO_2 Laser Line. Each spectrum is average of 100 spectra.

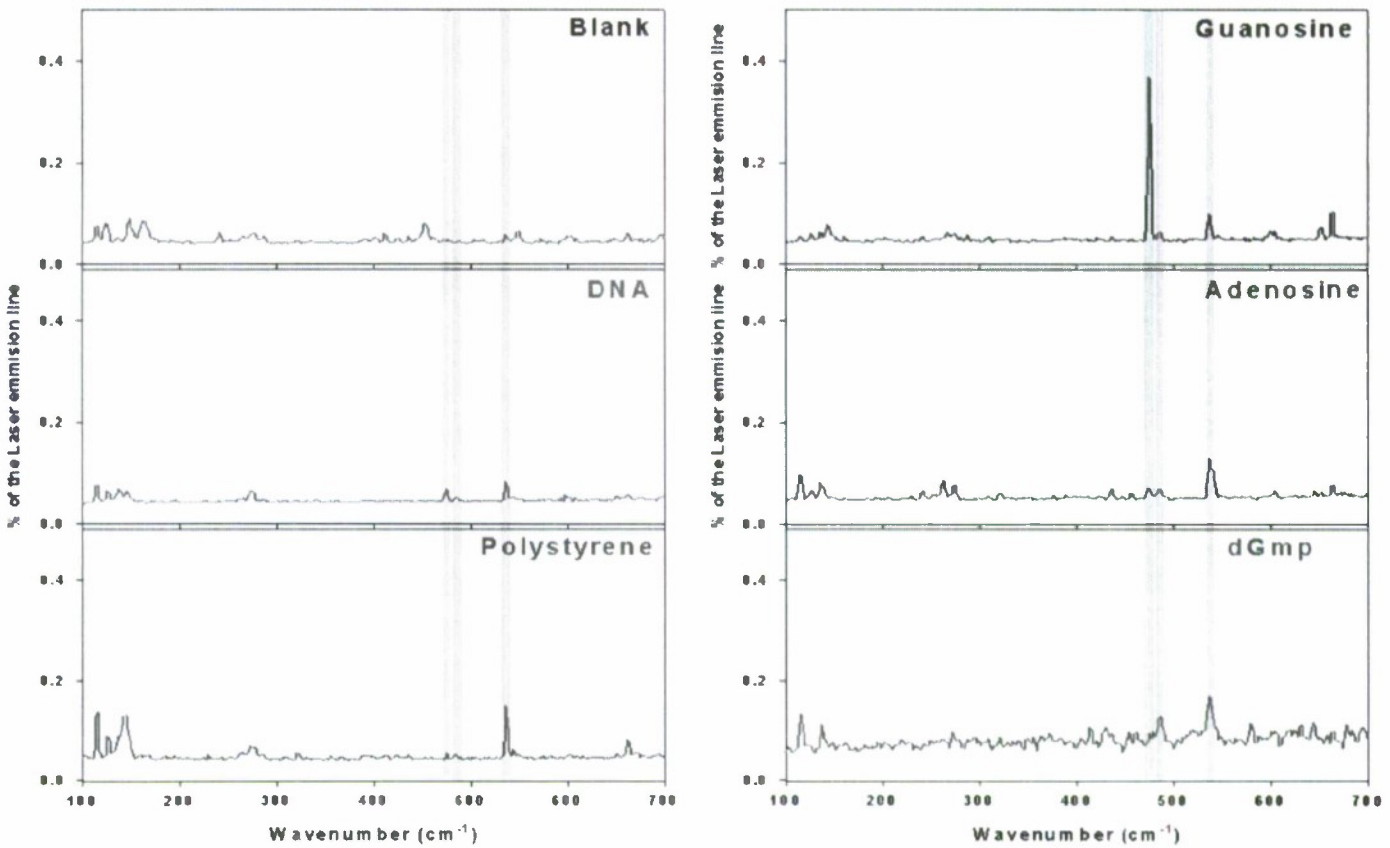

Figure 12. Estimated Emission/Transmission Spectra when Excited by a Scanning.

6. CONCLUSIONS

From the viewpoint of the quantum mechanics, a mixing of these two states occurs with large probability. Hence, the Fermi resonance provides a channel for a most effective transfer of energy. In our simulation, we identify numerous Fermi resonances in the region of our interest. Different transitions in DNA monophosphates including dAMP, dCMP, dGMP, and dTMP caused by anharmonicity transitions have been analyzed. The probabilities of transitions have been calculated, and the most effective channels of the energy transfer have been identified. The most important prediction of our research was as the first step to study the emission in the region of wavelength of the order 20 μm, which is twice larger than the wave length of the CO_2 laser operation.

In our experiment, we have detected a small emission line (no more than 2 % of the incident laser line intensity) at twice the wavelength for most of the DNA components. This finding may indicate occurrence of Fermi resonance. Therefore, these findings suggest that upon strong absorption of infrared radiation, DNA may emit MMW and/or sub-MMW radiation.

We recommend further investigation in modeling and experimental conformation of DNA absorption spectra and emission spectra at near MMW/SubMMW region.

Blank

LITERATURE CITED

1. Woolard, D.; Brown, E.; Pepper, M.; Kemp, M. Terahertz Frequency Sensing & Imaging: A Time of Reckoning Future Applications. *Proc. of IEEE* **2005**, *93(10)*.

2. Woolard, D. Terahertz *Electronic Research for Defense: Novel Technology and Science*. Presented at the 11th Int. Space Terahertz Tech. Symposium, Ann Arbor, MI, 2000; pp 22-38.

3. Woolard, D.L. et al. Millimeter Wave Induced Vibrational Modes in DNA as a Possible Alternative to Animal Tests to Probe for Carcinogenic Mutations. *J. App. Toxicol.* **1997**, *17*, pp 243-246.

4. Woodlard, D. L.; Loerop, W.R; Shur, M.S., Eds. *Terahertz Sensing Technology, Volume 1: Electronic Devices and Advanced Systems Technology*. Presented at the World Science Conference, Singapore, 2003.

5. Woodlard, D. L.; Loerop, W.R.; Shur, M.S., Eds. *Terahertz Sensing Technology, Volume 2: Emerging Scientific Applications & Novel Device Concepts*. Presented at the World Science Conference: Singapore, 2003.

6. Woolard, D.; Globus, T. Sensitivity Limits & Discrimination Capability of THz Transmission Spectroscopy as a Technique for Biological Agent Detection. In Proceedings of the *5th Joint Conference on Standoff Detection for Chemical and Biological Defense*; Williamsburg, VA, 2001.

7. Woolard, D.L.; Brown, E.R.; Samuels, A.C.; Globus, T.; Gelmont, B.; Wolski, M. Terahertz-frequency Remote-Sensing of Biological Warfare Agents. In *IEEE MTT-S International Microwave Symposium,* Philadelphia, PA, 2003, pp 763-766.

8. Globus, T.; Woolard, D.; Bykhovskaia, M.; Gelmont, B.; Werbos, L.; Samuels, A. *THz-Frequency Spectroscopic Sensing of DNA and Related Biological Materials* in *Terahertz Sensing Technology, Volume 2: Emerging Scientific Applications & Novel Device Concepts*; Woolard, D.L.; Loerop, W.R.; Shur, M.S., Eds.; World Science Conference, Singapore, 2003, pp 1-34.

9. Brown, E.R.; Bjarnason, J.E.; Chan, T.L.J.; Lee, A.W.M.; Celis, M.A. Optical Attenuation Signatures of Bacillus Subtillis in the THz Region. *App. Phys. Let.* **2004**, *84*, pp 3438-3440.

10. Woolard, D. L.; Globus, T.R.; Gelmont, B.L.; Bykhovskaia, M.; Samuels, A.C.; Cookmeyer, D.; Hesler, J.L.; Crowe, T.W.; Jensen, J.O.; Jensen, J.L.; Loerop, W.R. Submillimeter-Wave Phonon Modes in DNA Macromolecules. *Physical Review E.* **2002,** *65*, pp 1903-1914.

11. Brown, E.R.; Woolard, D.L.; Samuels, A.C.; Globus, T.; Gelmont, B. Remote Detection of Bioparticles in the THz Region. In Proceedings of the International Microwave Symposium, Seattle, WA, 2002.

12. Woolard, D. L., et al. *Terahertz-Frequency Spectroscopy as A Technique for the Remote Detection of Biological Warfare Agents.* In the proceedings of the 23rd Army Science Conference, Orlando, FL, 2002.

13. Frisch, M. J., et al. *Gaussion Software Package.* Gaussian, Inc.: Pittsburgh, PA, 2002.

14. Born, M.; Huang, K. *Dynamical Theory of Crystal Lattices*; Oxford at the Clarendon: Oxford, 1954.

APPENDIX

NONPARABOLICITY

As the first approach to the finding of the largest nonparabolic contribution, we studied the atoms with the largest amplitudes of vibrations. Expectedly the lightest of atoms, hydrogen, provided the largest amplitudes of vibrations. Hydrogen in monophosphates is connected with carbon, oxygen, or nitrogen. For the estimate of effects of nonparabolicity, we have taken into account the stretching of the bonds, which has the largest rigidity. For carbon - hydrogen (C-H) bond, we have chosen the methane to calculate the third derivative of the potential near potential minimum. The potential energy curve (PEC) of methane as a function of bond length of four C-H bonds is shown in Figure1 where the insets are strueture of methane (left) and the PEC around the minimum (right). Bond lengths of four C-H bonds are changed simultaneously during the calculation. Morse potential is used to regress the PEC and to ealculate the third derivative of the potential at the minimum

$$V(r) = V(r_0) + D\{1 - \exp(-q(r - r_0))\}^2$$

where r_0 is thc equilibrium length of bond. We have found the following Morse paramcters for thc methane

$V(r_0)$=-40.2 H, D=0.877 H, r_0=1.08 A, q=1.79 A^{-1}

When applying these results to the analysis of a single bond it is necessary to divide energies over four bonds of the methane.

Methanol was chosen for oxygen – hydrogen (O-H) bond. The PEC of methanol as a funetion of bond length of O-H is shown in Figure 2 where the inset is the structure of methanol. Morse potential is applied again to regress the PEC and to calculate the third derivative of the potential at the minimum. We have found the following Morse parameters for methanol

$V(r_0)$=-115.0 H, D= 0.141 H, r_0=0.93 A, q=2.85 A^{-1}.

The O-H bond was found to have twice bigger third derivative than C-H bond. Hencc we have taken for nitrogen – hydrogcn (N-H) bond the smaller value of the C-H bond

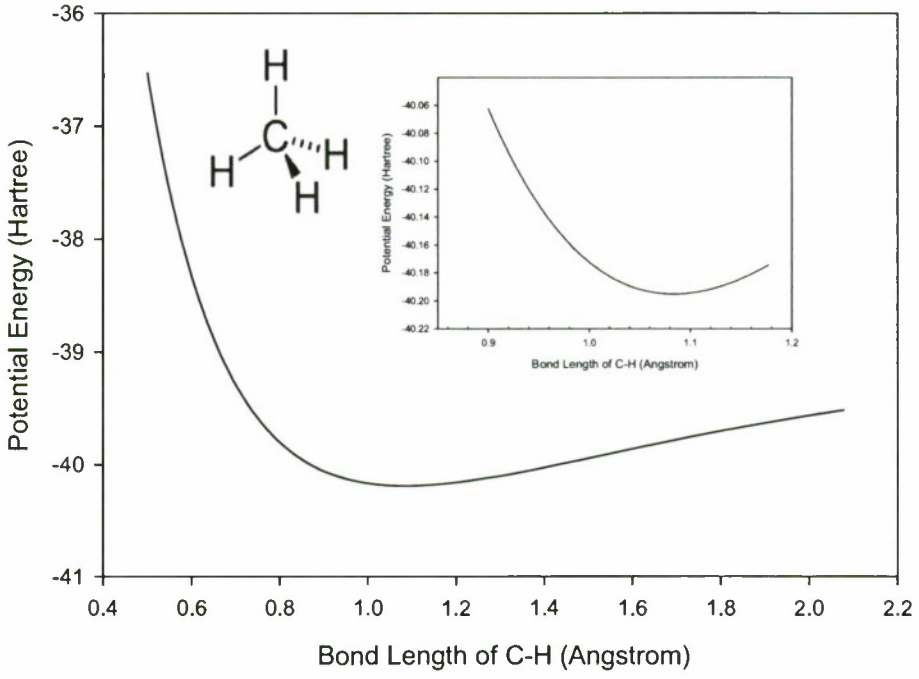

Figure 1. Potential Energy Curve of Methane as a Function of Bond Length of Four C-H Bonds Calculated with HF/6-31G(d) Method in G98 Package.

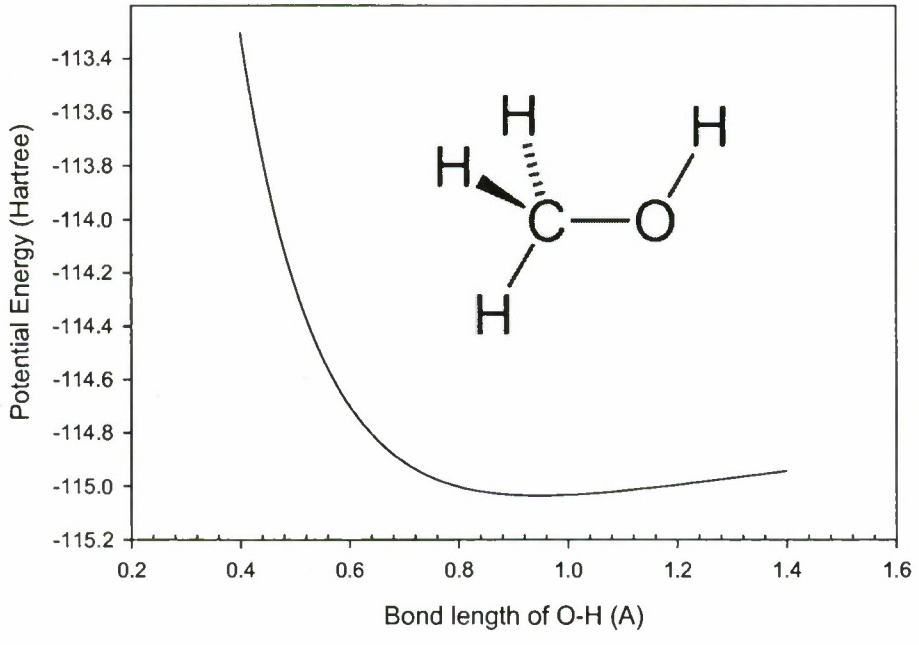

Figure 2. Potential Energy Curve of Methanol as a Function of Bond Length of O-H Bonds Calculated with HF/6-31G(d) Method in G98 Package.